Electronic Supplementary Material (ESI) for Materials Chemistry Frontiers.
This journal is © the Partner Organisations 2017

Electronic Supplementary Information

Janus Quantum Dot Vesicles Generated through Membrane Fusion

Huimei Li, Aidi Zhang, Ke Li, Wei Huang, Yiyong Mai, Yongfeng Zhou*, Deyue Yan*

School of Chemistry and Chemical Engineering, State Key Laboratory of Metal Matrix Composites, Shanghai Key Laboratory of Electrical Insulation and Thermal Ageing, Shanghai Jiao Tong University, 800 Dongchuan Road, Shanghai 200240, China
E-mail: mai@sjtu.edu.cn; yfzhou@sjtu.edu.cn

1. Experimental section

1.1 *Materials*

Triethylamine (TEA) and tetrahydrofuran (THF) (AR grade, Shanghai Chemical Reagent Co.) were refluxed with CaH_2 and then distilled prior to use. 1-adamantanecarbonyl chloride (>99% pure), iron chloride ($FeCl_3 \cdot 6H_2O$, 97%), oleic acid (90%), 1-octadecene (90%) were purchased from Aldrich and used as received. Sodium oleate (95%) was purchased from TCI. All the other chemical reagents were purchased from Shanghai Chemical Reagent Co.

1.2 *Synthesis of HBPO and HBPO-star-PEOs*

Three HBPO-star-PEO samples (HBPO-star-PEO_2, HBPO-star-PEO_4 and HBPO-star-PEO_{10}) were synthesized through cationic ring-opening polymerization (CROP) according to our previous method (Figure S1).[1,2] The polymers have the same HBPO cores and different molar ratios of the PEO arms to the HBPO core ($R_{A/C}$).

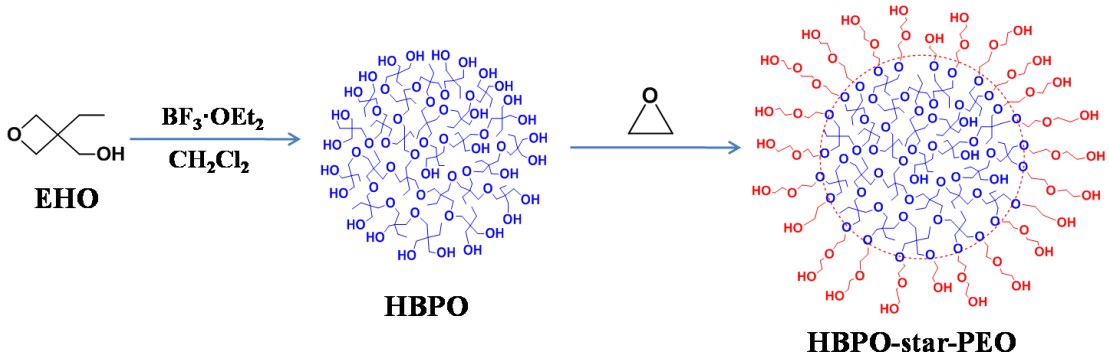

Figure S1 The synthetic scheme of HBPO-star-PEO.

1.3 *Synthesis of HBPO-star-PEO-CD and HBPO-star-PEO-Ada*

The synthetic process of HBPO-star-PEO-CD includes two steps. In step 1, HBPO-star-PEO_2 with $R_{A/C}$ = 2 was reacted with butanedioic anhydride to obtain the carboxyl-terminated polymers (HBPO-star-PEO-COOH). In step 2, the carboxyl groups in HBPO-star-PEO-COOH were further reacted with the hydroxyl groups in β-CD through the esterification reaction to obtain the final CD-functionalized polymer of HBPO-star-PEO-CD (Figure S2). The detailed syntheses of HBPO-star-PEO-CD were shown in our previously reported literature.[3]

The synthetic process of HBPO-star-PEO-Ada is shown in Figure S3. HBPO-star-PEO_4 with $R_{A/C}$ = 4 was dissolved in chloroform solvent, and 1-adamantanecarbonyl chloride was dropped into the solution slowly, then the solution was kept stirring for 24 h at room temperature. The detailed syntheses were shown in our previously reported literature.[4]

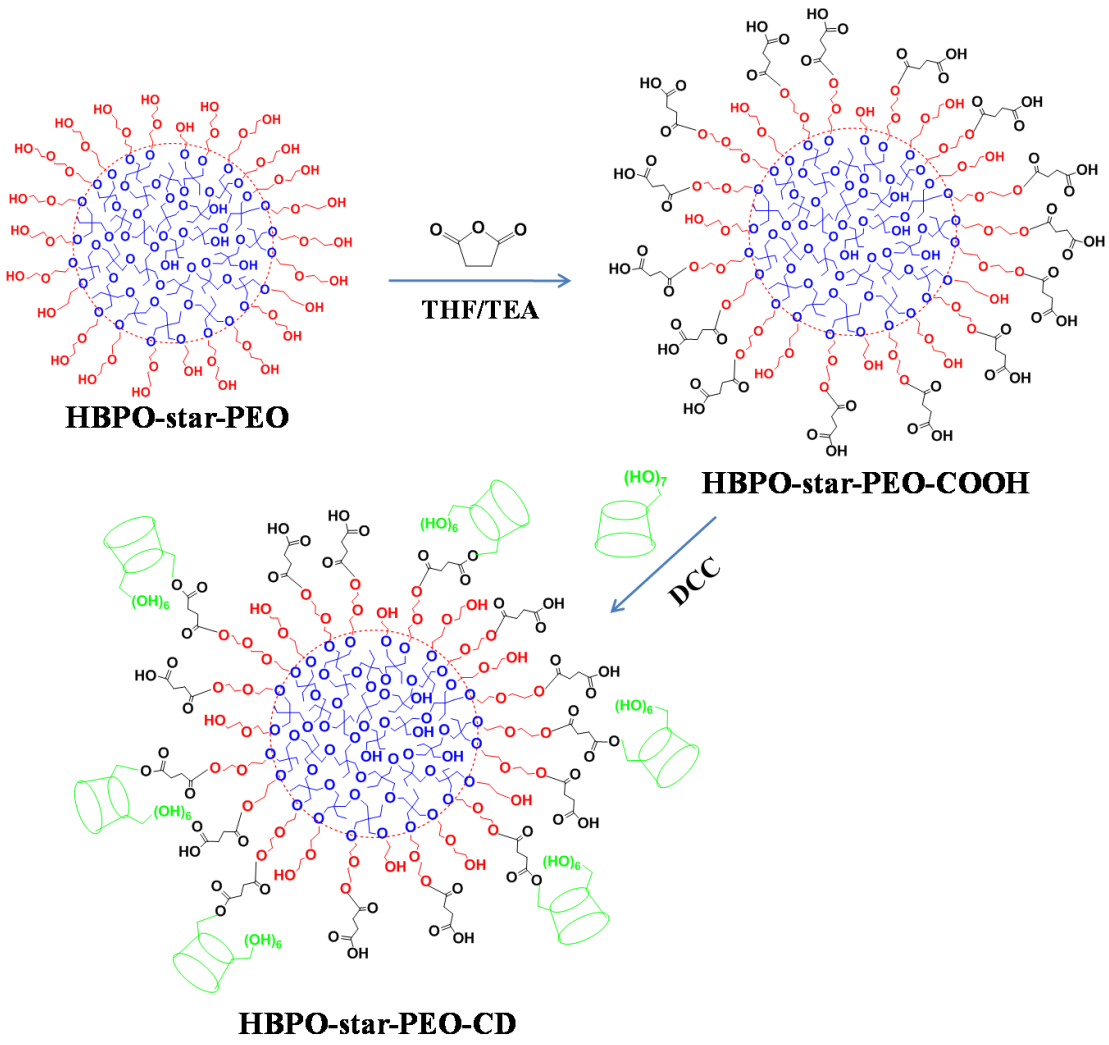

Figure S2 The synthetic scheme of HBPO-star-PEO-CD.

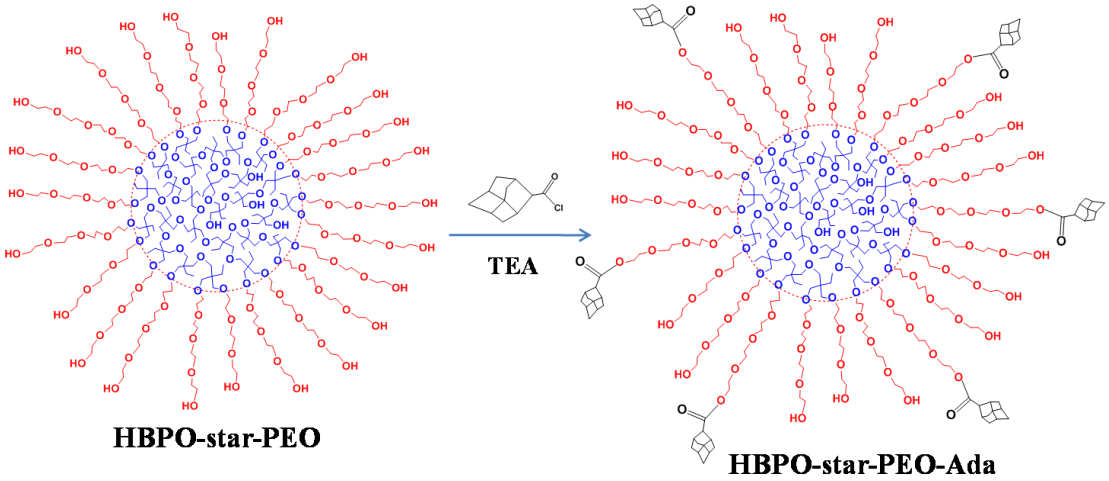

Figure S3 The synthetic scheme of HBPO-star-PEO-Ada.

1.4 *Synthesis of QDs*

Fe_3O_4 nanoparticles were synthesized using oleic acid as the stabilizing agent

according to a previously reported literature method.[5-7] Briefly, 1.5 g of iron chloride ($FeCl_3$ $6H_2O$, 5.5 mmol) and 5.2 g of sodium oleate (17 mmol) were first added in a 100 mL flask. Then, 20 mL of hexane, 11.5 mL of ethanol, and 8.8 mL of distilled water were added to the flask. The mixture was heated to 70 ℃ and reflux at this temperature for four hours, which produced iron-oleate in the organic layer. The organic layer was washed with 30 mL of water for three times and then separated by centrifugation (8,000 rpm, 10 minutes). Subsequently, hexane was removed from the organic mixture by rotor evaporation and the remnant iron-oleate was kept under vacuum overnight (about 12 hours). The synthesis of iron oxide nanoparticles was carried out by reacting 5.5 g of iron-oleate and 1.5 g of oleic acid (5.3 mmol) in 31 g of 1-octadecene in a 100 mL round-bottom flask. The reaction mixture was heated to 320 ℃ at a rate of 200 ℃/hour, and then kept at the temperature for 30 minutes, with the color turning from dark brown to black upon the formation of nanoparticles. The resulting mixture was cooled down to the room temperature and the nanoparticles were precipitated by adding ethanol (35 mL). The precipitate was collected by centrifugation (8,000 rpm, 10 minutes) and then redispersed in hexane (10 mL). The nanoparticles were further purified by the addition of acetone (35 mL), centrifugation (8,000 rpm, 10 minutes), and redispersion in hexane (10 mL). The acetone wash was repeated two more times. Afterward, the nanoparticles were dissolved in chloroform (10 mL) and centrifuged at a low speed of 3,000 rpm for 5 minutes to remove the possible nanoparticle aggregates. Finally, chloroform was removed by rotary evaporation and the resultant nanoparticles were weighed and redispersed in THF (5

mg/mL). The thermogravimetric analysis (TGA) revealed ~31 % weight percentage for the iron oxide in the dried sample and ~69 % for the oleic acid ligand (Figure S4).

CdSe/CdS QDs were synthesized in a previous work[8] and provided by Dr. Aidi Zhang (the second author of this paper). The concentration of the CdSe/CdS QDs in tetrahydrofuran (THF) was 1×10^{-4} mol/L, which was determined by the Lambert–Beer's law as described in the literature.[9] (Zn)CuInS/ZnS QDs with a typical concentration of 1×10^{-4} mol/L in THF were prepared in a previous work[10] and supplied by Dr. Aidi Zhang.

1.5 *Preparation of QBP-1 by co-self-assembly of HBPO-star-PEO, HBPO-star-PEO$_2$-CD and CdSe/CdS QDs*

Table S1. Recipes of QBPs and JQBPs

Sample	Recipe[a]
QBP-1	HBPO-star-PEO_2 + HBPO-star-PEO_{10} + HBPO-star-PEO_2-CD + CdSe/CdS (molar ratio: 10:1.4:3.4:1)
QBP-2	HBPO-star-PEO_2 +HBPO-star-PEO_{10} + HBPO-star-PEO_4-Ada + (Zn)CuInS/ZnS (molar ratio: 2.5:0.35:0.5:1)
QBP-3	HBPO-star-PEO_2 + HBPO-star-PEO_{10} + HBPO-star-PEO_4-Ada + Fe_3O_4 (molar ratio: 16.7:2.3:3.3:1)
JQBP-1	QBP-1 + QBP-2
JQBP-2	QBP-1 + QBP-3

[a] The subscript of PEO represents the molar ratio of the PEO arms to the HBPO core ($R_{A/C}$). For example, in HBPO-star-PEO_2, the subscript 2 represents $R_{A/C}$=2.

The preparation of QBP-1 followed the recipe in Table S1. Typically, 30 mg HBPO-star-PEO_2 (the subscript expresses the molar ratio of the PEO arms to the HBPO core), 10 mg HBPO-star-PEO_{10}, and 10 mg HBPO-star-PEO_2-CD were mixed together in THF and the mixture was stirred at room temperature for 30 minutes. Then 5 μL THF dispersion (1×10^{-4} mol/L) of CdSe/CdS QDs was added into the mixture and then stirred for another 30 minutes. Afterwards, the organic solvents were

removed by rotary evaporation, leaving behind a uniform hyperbranched polymer/QDs hybrid film. Then, 5 mL distilled water was added and the film was immersed in water for 30 minutes. The film rehydration induced the co-self-assembly of the hyperbranched polymers and the QDs.

1.6 ***Preparation of QBP-2 by co-self-assembly of HBPO-star-PEO, HBPO-star-PEO$_4$-Ada and (Zn)CuInS/ZnS QDs***

A similar method was used to prepare QBP-2. Typically, 30 mg HBPO-star-PEO_2, 10 mg HBPO-star-PEO_{10}, and 10 mg HBPO-star-PEO_4-Ada were mixed together in THF. Then 20 μL THF dispersion (1×10^{-4} mol/L) of (Zn)CuInS/ZnS QDs was added into the solution and the mixture was stirred for 30 minutes. Afterwards, the organic solvents were removed by rotary evaporation, leaving behind a hyperbranched polymer/QDs hybrid film. Then 5 mL distilled water was added and the film was immersed in water for 30 minutes to induce the co-self-assembly of the hyperbranched polymers and the (Zn)CuInS/ZnS QDs.

1.7 ***Preparation of QBP-3 by co-self-assembly of HBPO-star-PEO, HBPO-star-PEO$_4$-Ada and Fe_3O_4 nanoparticles***

Similarly, 30 mg HBPO-star-PEO_2, 10 mg HBPO-star-PEO_{10}, and 10 mg HBPO-star-PEO_4-Ada were mixed together in THF. Then 50 μL THF dispersion (5 mg/mL) of Fe_3O_4 was added into the solution and the mixture was stirred for 30 minutes. Afterwards, the organic solvents were removed by rotary evaporation. Then 5 mL distilled water was added and the film was immersed in water for 30 minutes to induce the co-self-assembly of the hyperbranched polymers and Fe_3O_4.

1.8 *Formation of JQBPs*

For preparing JQBP-1, 1 mL aqueous solution of QBP-1 and 1 mL aqueous solution of QBP-2 were mixed and then stirred gently for over 6 hours. The real-time observation was carried out after the mixing for 30 minutes. The mixed solution was dropped on a glass slide and then observed directly under an optical/fluorescence microscope. For JQBP-2, the same approach was applied for the preparation and the real-time observation.

2. Characterizations

Liquid-phase Nuclear Magnetic Resonance (^{1}H NMR and ^{13}C NMR) was performed on a Varian Mercury Plus 400-MHz spectrometer using deuterated dimethyl sulfoxide (DMSO-d_6) or $CDCl_3$ as solvents at 20 ^{o}C, and tetramethylsilane (TMS) was used as the internal reference. Gel permeation chromatography (GPC) was performed on a Perkin-Elmer series 200 system (10 μm PL gel 300 × 7.5 mm mixed-B and mixed-C columns, linear PMMA calibration) equipped with a refractive index (RI) detector. THF was used as the eluent at a flow rate of 1 mL/min at 70 ℃. Thermogravimetric analysis (TGA) experiments were performed on PerkinElmer TGA 7, made by Perkin Elmer, Inc., USA. The samples were measured under an oxygen atmosphere. Photoluminescence (PL) spectra were recorded on a QC-4-CW spectrometer, made by Photon Technology International, Int. USA/CAN. Ultraviolet-visible absorption spectrum (UV/Vis) spectra were performed on a Lambda 750S spectrometer, made by Perkin Elmer, Inc., USA. The scanning range of the spectra was form 250 nm to 750 nm with 2 nm slit. The scanning rate was set at

480 nm/min. Transmission electron microscopy (TEM) studies were performed with a JEOL JEM-100CX-II instrument at a voltage of 200 kV. Samples were prepared by drop-casting vesicle solutions onto carbon-coated copper grids and then air-drying at room temperature before measurement. The morphologies of the vesicles were observed by an optical/fluorescence microscope (Leica DM4500 B). Fluorescence micrographs of QBP-1 were recorded upon blue or purple light excitation with exposure time of 2 seconds; fluorescence micrographs of QBP-2 were recorded upon blue light excitation with exposure time of 4 seconds; fluorescence micrographs of QBP-3 were recorded upon purple light excitation with exposure time of 5 seconds.

2.1 *TGA curves of Fe_3O_4*

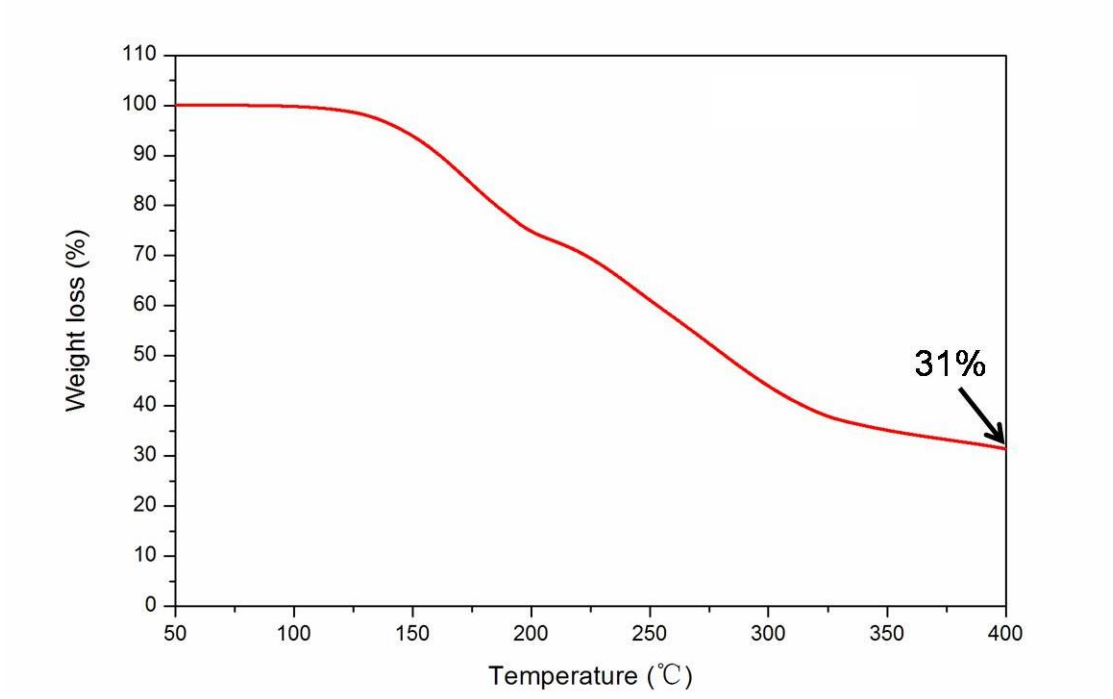

Figure S4. TGA curves of Fe_3O_4.

2.2 *Characterizations of HBPO and HBPO-star-PEOs*

The polymers have the same HBPO cores with the number-average molecular weight (Mn) of about 4,200 according to GPC and degree of branching (DB) of 42%

(Fig. S5). The molar ratios of the PEO arms to the HBPO core ($R_{A/C}$) for the three polymers is 2, 4 and 10, respectively (Figs. S6-S8). The M_n of the HBPO-star-PEOs measured by GPC is about 6,000, 9,100 and 14,000, respectively (Fig. S9).

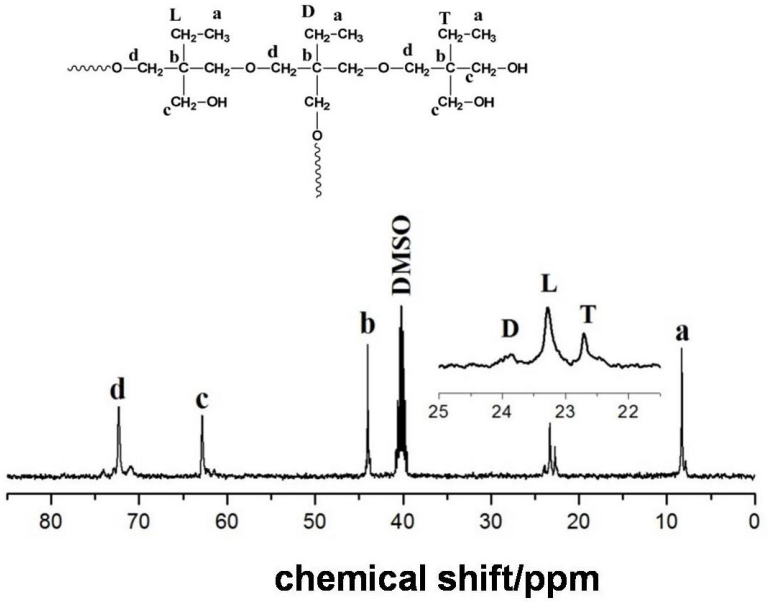

Figure S5. Quantitative ^{13}C NMR spectrum of HBPO.

The quantitative ^{13}C NMR spectra of HBPO samples is given in Figure S5, in which the three peaks near 22-25 ppm are attributed to the carbon atoms of methylene in the ethyl groups of the dendritic unit (D), the linear unit (L), and the terminal unit (T). The degree of branching (DB) of the HBPO core is calculated according to the equation of DB = $(S_D+S_T)/(S_D+S_L+S_T)$, where S represents the integral area of the corresponding peak; thus DB is about 42%.

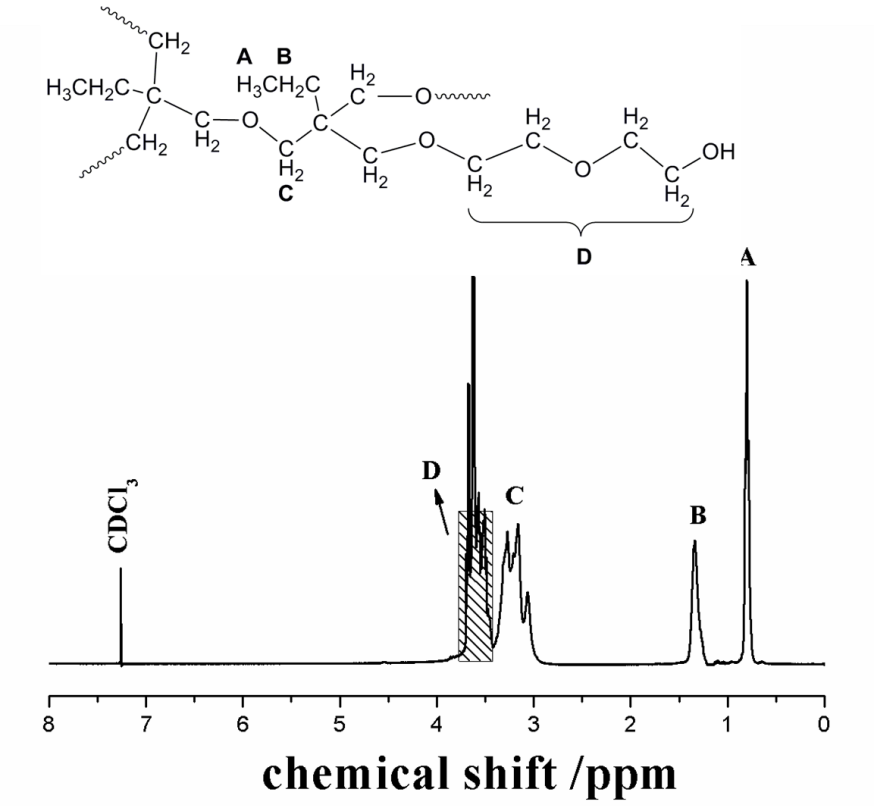

Figure S6. ^{1}H NMR spectrum of HBPO-star-PEO$_2$. $R_{A/C}$= (S_D/4) / (S_A/3) = 3S_D/4S_A = ~2.

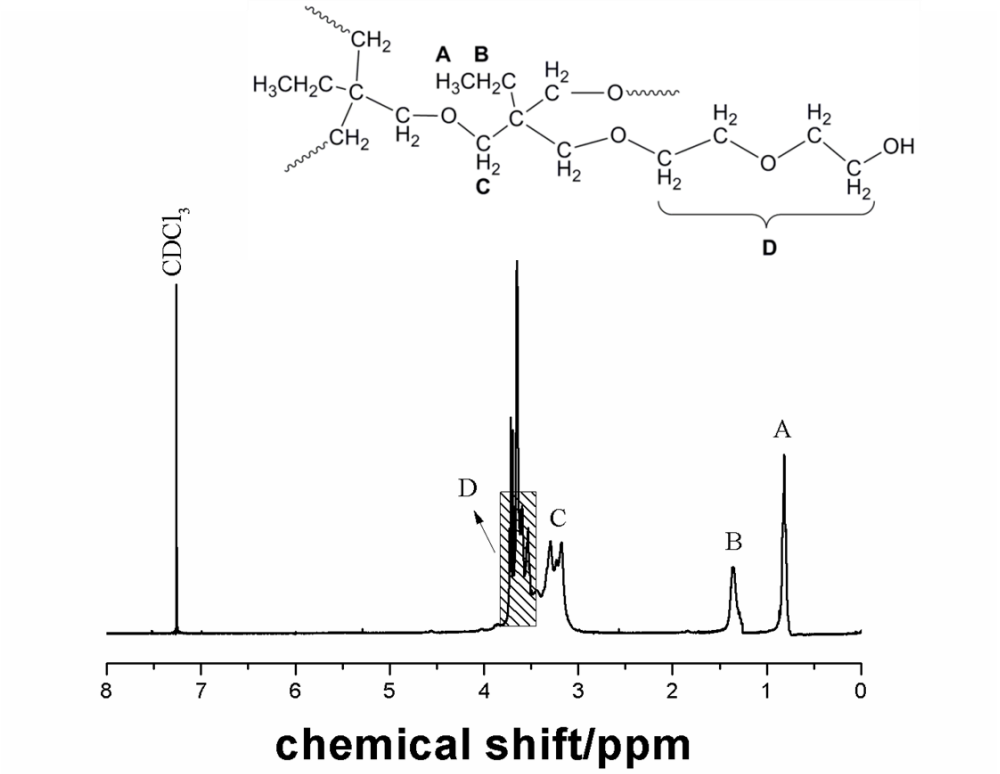

Figure S7. ^{1}H NMR spectrum of HBPO-star-PEO$_4$. $R_{A/C}$= (S_D/4) / (S_A/3) = 3S_D/4S_A = ~4.

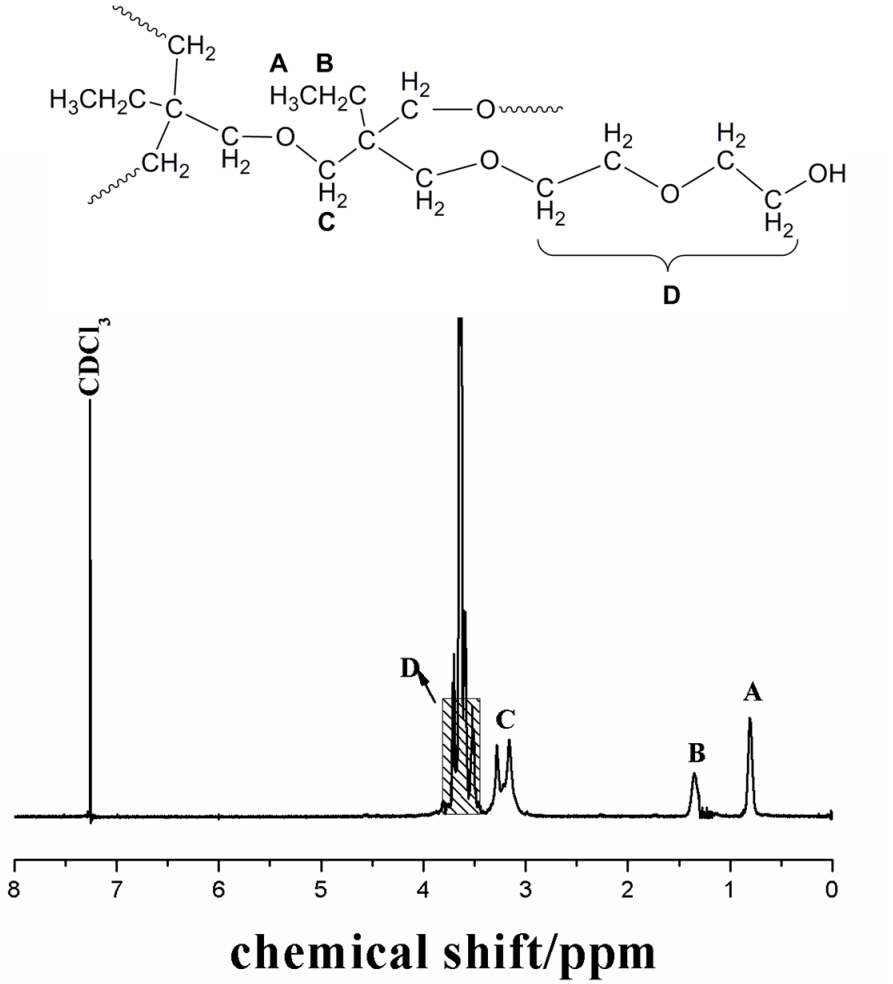

Figure S8. ^{1}H NMR spectrum of HBPO-star-PEO$_{10}$. $R_{A/C}$= (S_D/4) / (S_A/3) = 3S_D/4S_A = ~10.

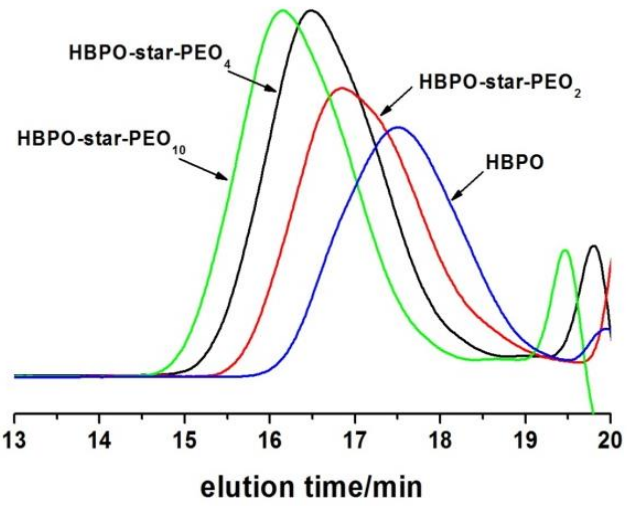

Figure S9. GPC curves of HBPO-star-PEO$_2$, HBPO-star-PEO$_4$, HBPO-star-PEO$_{10}$ and the corresponding HBPO core.

2.3 *^{1}H NMR spectrum of HBPO-star-PEO-CD*

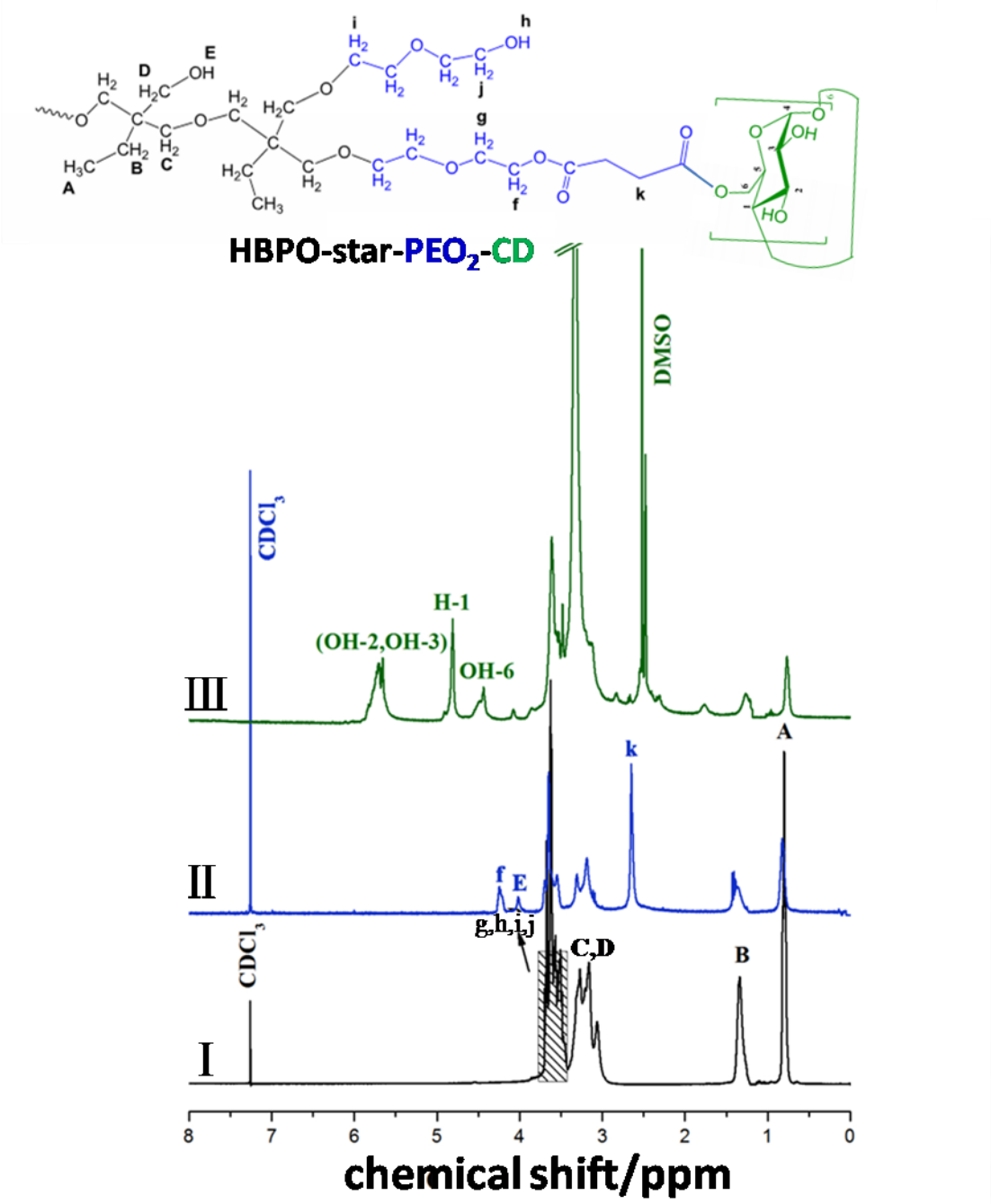

Figure S10. ^{1}H NMR spectra of HBPO-star-PEO$_2$ (Ⅰ), HBPO-star-PEO$_2$-COOH (Ⅱ) and HBPO-star-PEO$_2$-CD (Ⅲ).

The ^{1}H NMR spectra of HBPO-star-PEO$_2$, HBPO-star-PEO$_2$-COOH and HBPO-star-PEO$_2$-CD with assignments (symbols A-E represent the signals from the

HBPO core, and symbols f-k represent the signals from PEO arms) are shown in Figure S10. Compared with that of HBPO-star-PEO_2, the ^{1}H NMR spectrum of HBPO-star-PEO_2-COOH shows new signals appeared at 2.64 ppm (-CH2- groups from butanedioic anhydride, protons k) and 4.24 ppm (protons f), which confirmed the successful carboxylation of HBPO-star-PEO_2. The conversion ratio from hydroxyl groups to carboxyl groups could be calculated by comparing the integral area of peak f with that of peak A ($3S_f/2S_A$), and the result is ~57%. Compared with that of HBPO-star-PEO_2-COOH, the ^{1}H NMR spectrum of HBPO-star-PEO_2-CD shows the new signals appeared at 4.47 ppm, 4.80 ppm and 5.75 ppm attributed to the protons from β-CD. These results both confirm that β-CD was grafted successfully to the surface of HBPO-star-PEO_2-COOH through the formation of ester bondings. The grafting percentage of the CD group is approximately 11%.

2.4 *^{1}H NMR spectra of HBPO-star-PEO-Ada*

The ^{1}H NMR spectra of HBPO-star-PEO_4 and HBPO-star-PEO_4-Ada are shown in Figure S11. Comparing the ^{1}H NMR spectra of HBPO-star-PEO_4 with that of HBPO-star-PEO_4-Ada, some new proton signals appeared at 4.18 ppm (proton f) and 1.6-2.1 ppm (protons a-c) in the spectrum of HBPO-star-PEO-Ada, which confirmed that adamantane was grafted successfully through the formation of ester bonding. The adamantane percent grafting calculated by comparing the integral area of peak f with that of peak A ($3S_f/2S_A$) is about 15%.

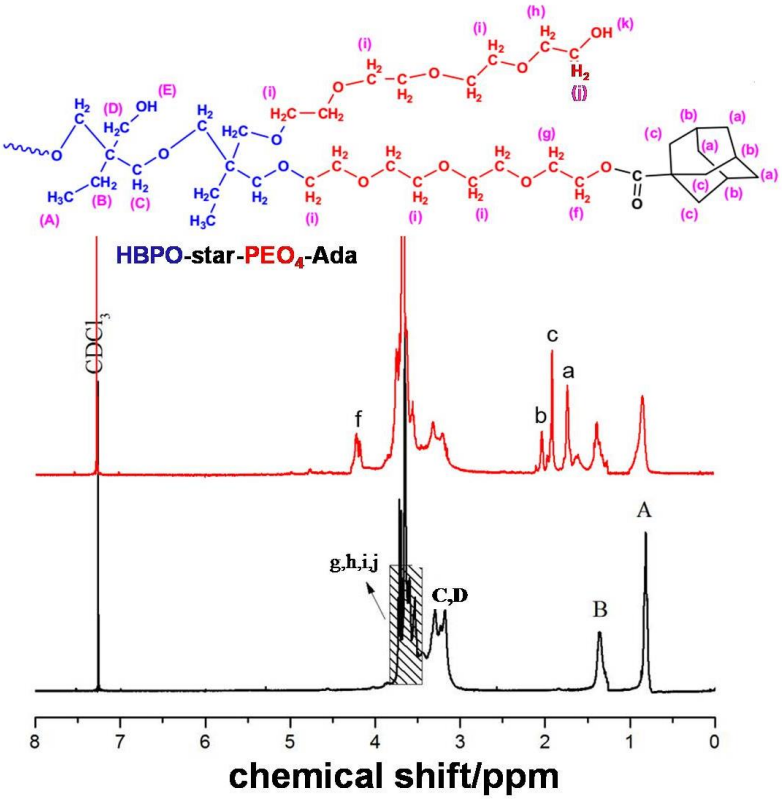

Figure S11. ^{1}H NMR spectra of HBPO-star-PEO_4-Ada (up) and HBPO-star-PEO_4 (down).

2.5 *Characterizations of the QDs*

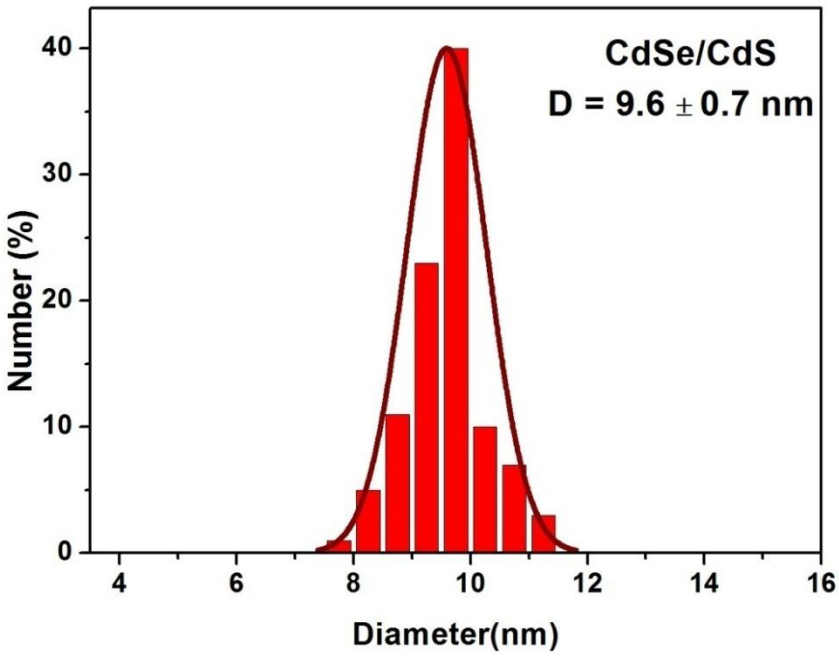

Figure S12. Particle distribution histogram for CdSe/CdS QDs based on statistics of particles in TEM images.

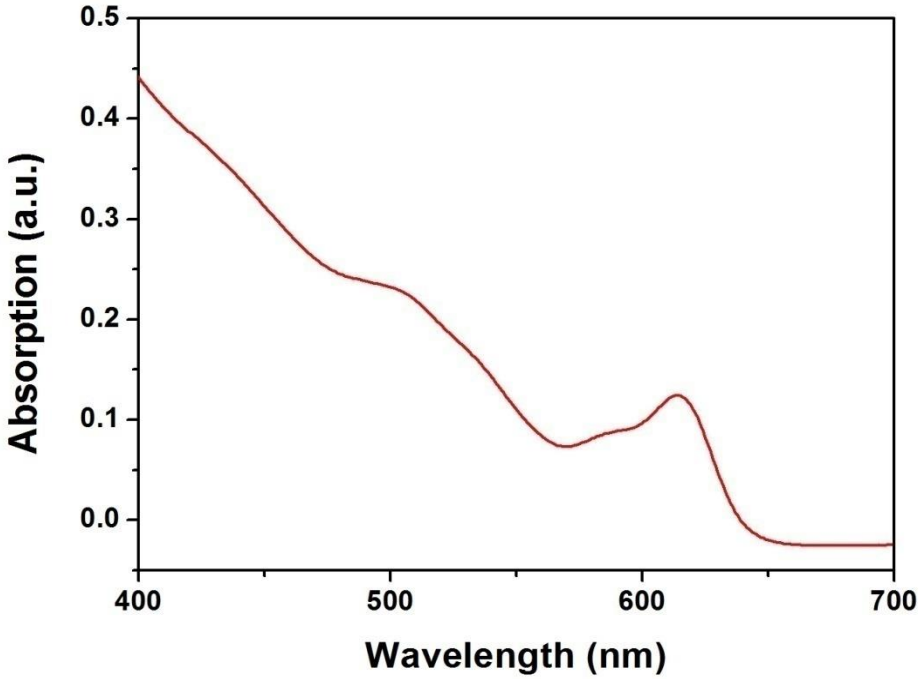

Figure S13. UV-Vis spectrum of CdSe/CdS QDs in THF.

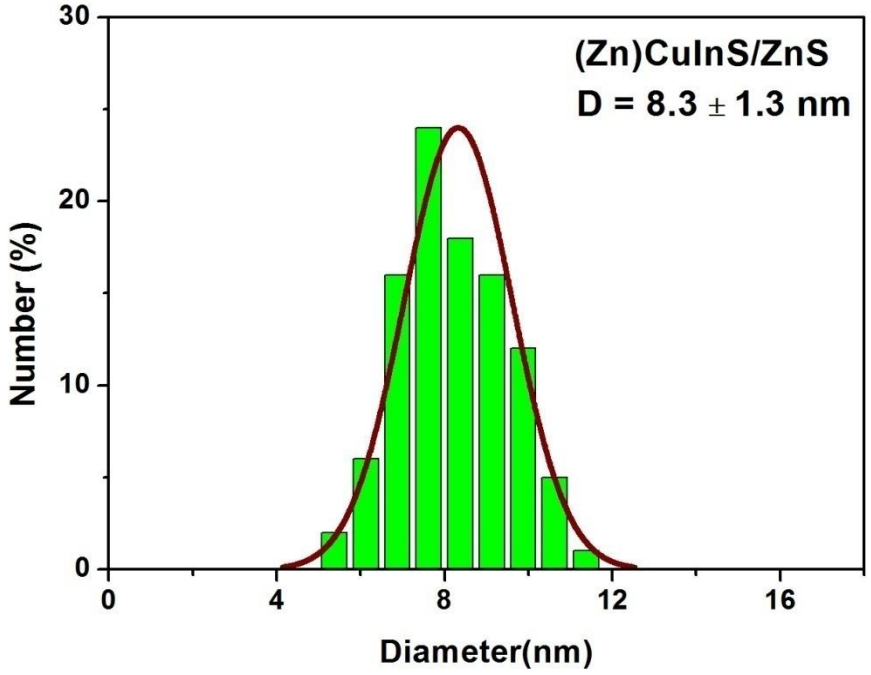

Figure S14. Particle distribution histogram for (Zn)CuInS/ZnS QDs based on statistics of particles in TEM images.

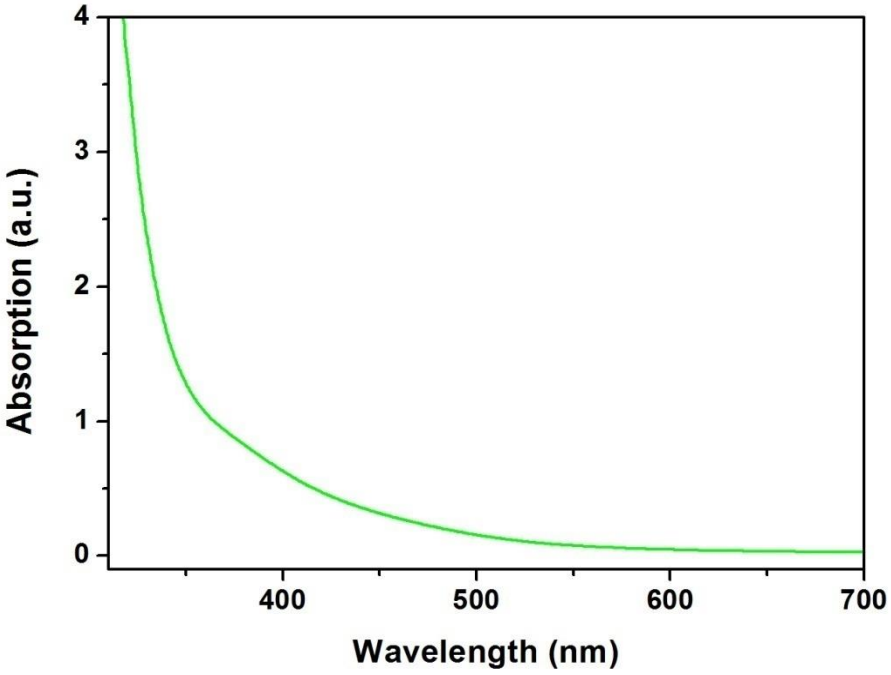

Figure S15. UV-Vis spectrum of (Zn)CuInS/ZnS QDs in THF.

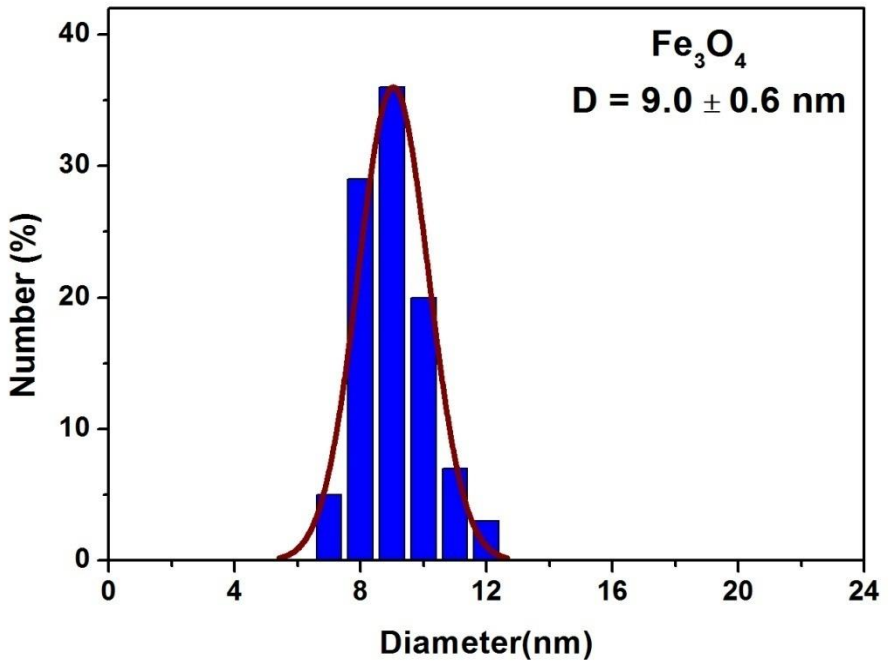

Figure S16. Particle distribution histogram for Fe_3O_4 nanoparticles based on statistics of particles in TEM images.

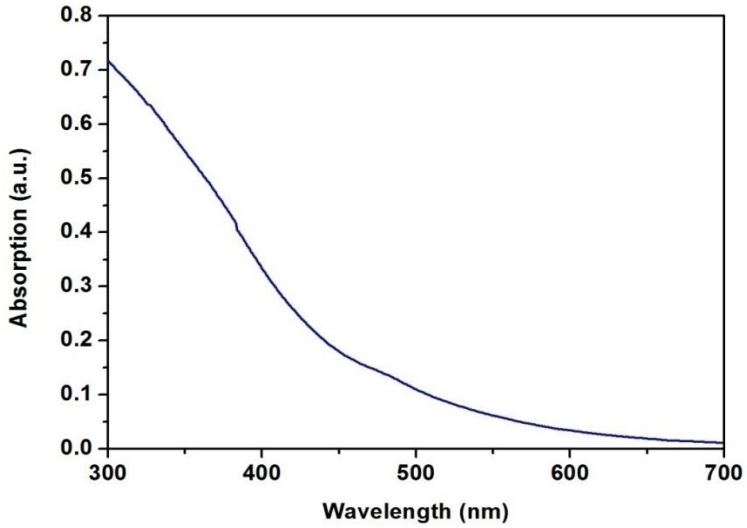

Figure S17. UV-Vis spectrum of Fe_3O_4 nanoparticles in THF.

2.6 *Characterizations of QBPs*

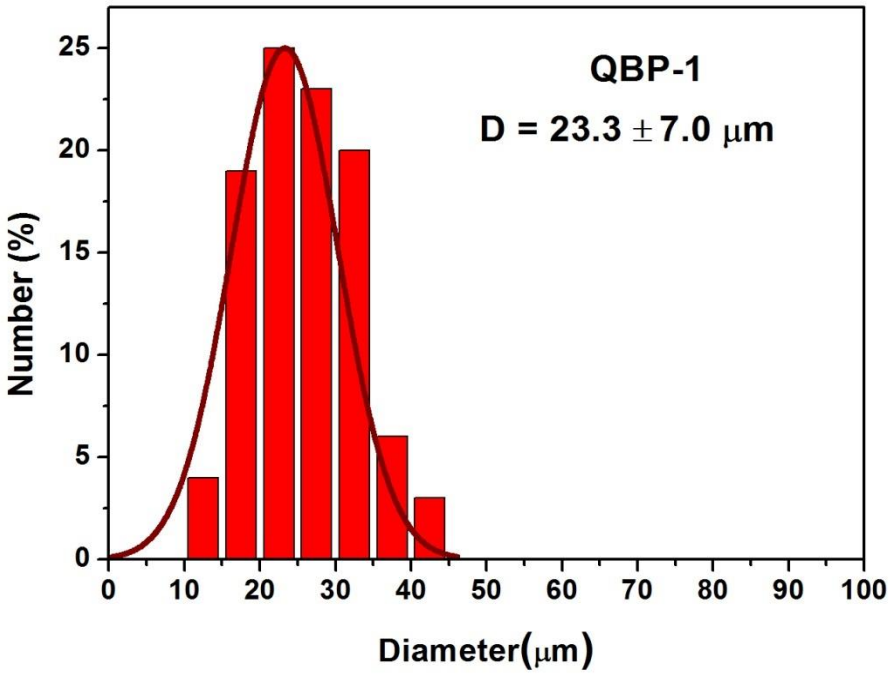

Figure S18. Size distribution of QBP-1 from the statistics of the vesicles in optical photographs.

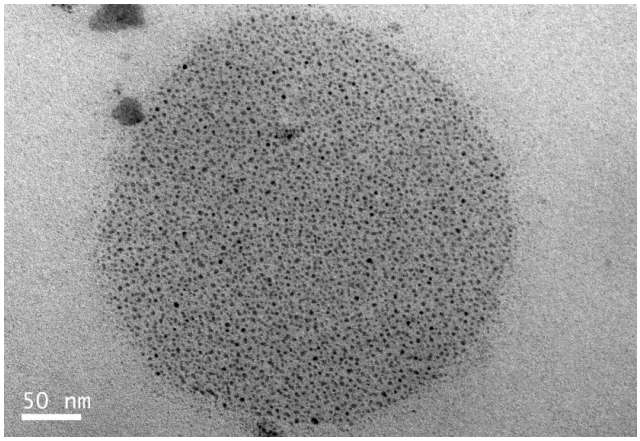

Figure S19. TEM image of QBP-2.

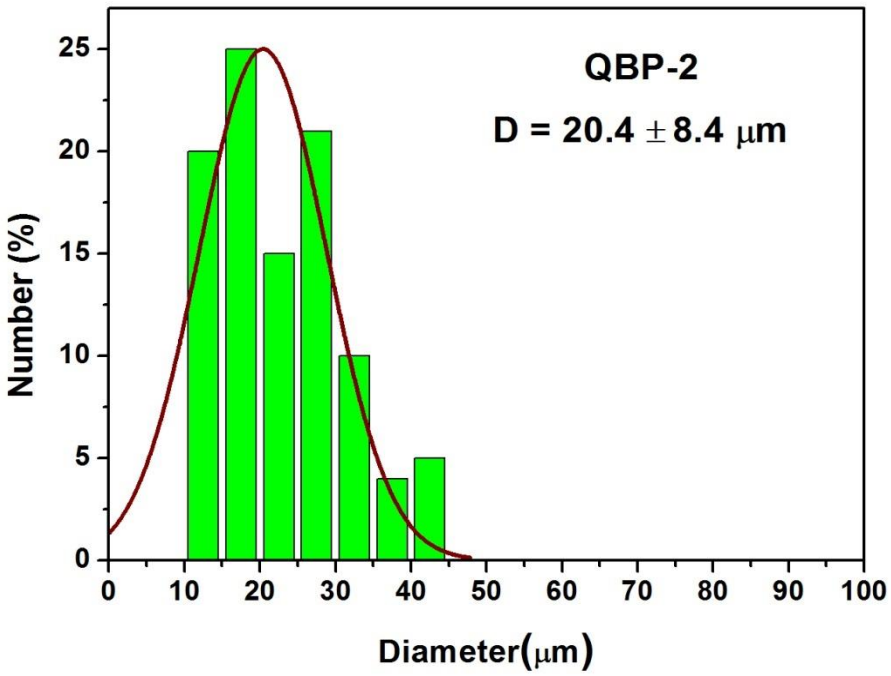

Figure S20. Size distribution of QBP-2 from the statistics of the vesicles in optical photographs.

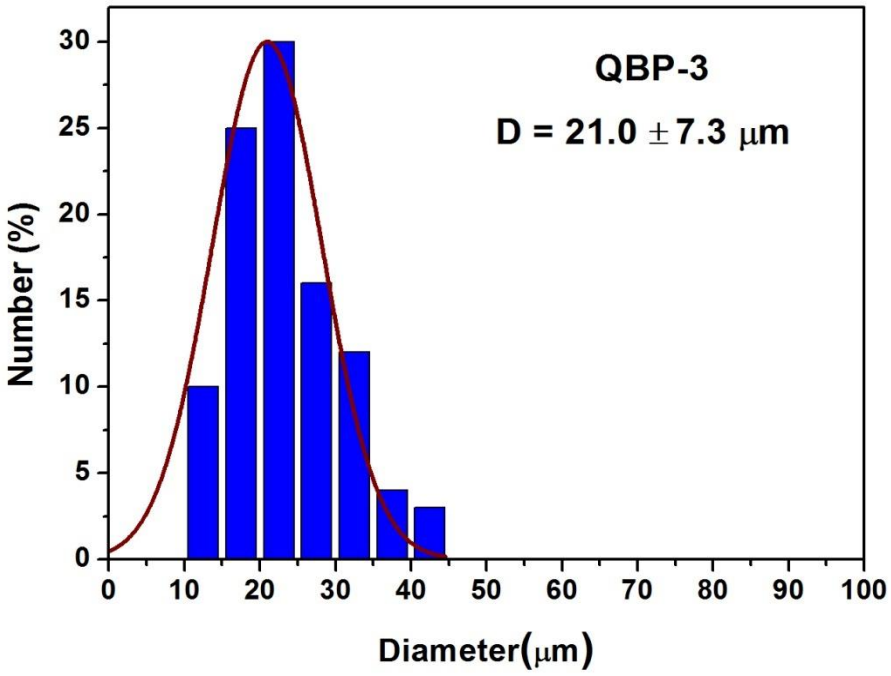

Figure S21. Size distribution of QBP-3 from the statistics of the vesicles in optical photographs.

2.7 *Characterizations of JQBPs*

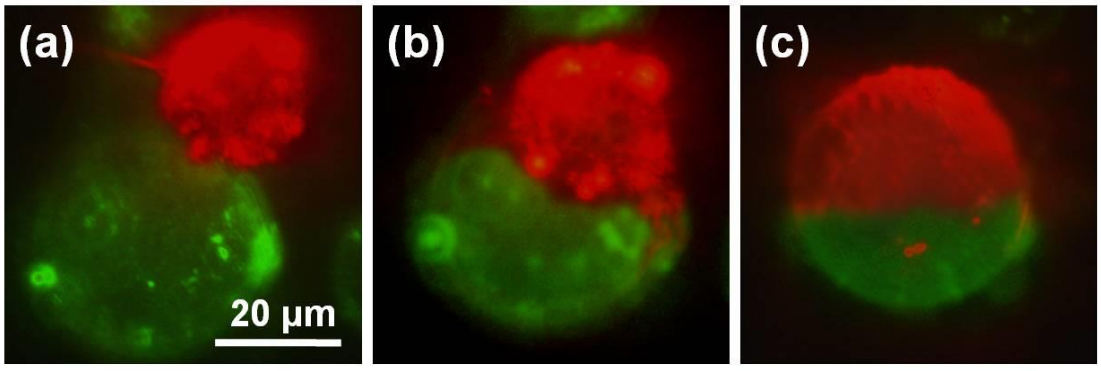

Figure S22. Real-time vesicle fusion process tracked under a fluorescence microscope of JQBP-1 by mixing the QBP-1 and QBP-2 solutions. (a) 0 second; (b) 35 seconds; (c) 110 seconds.

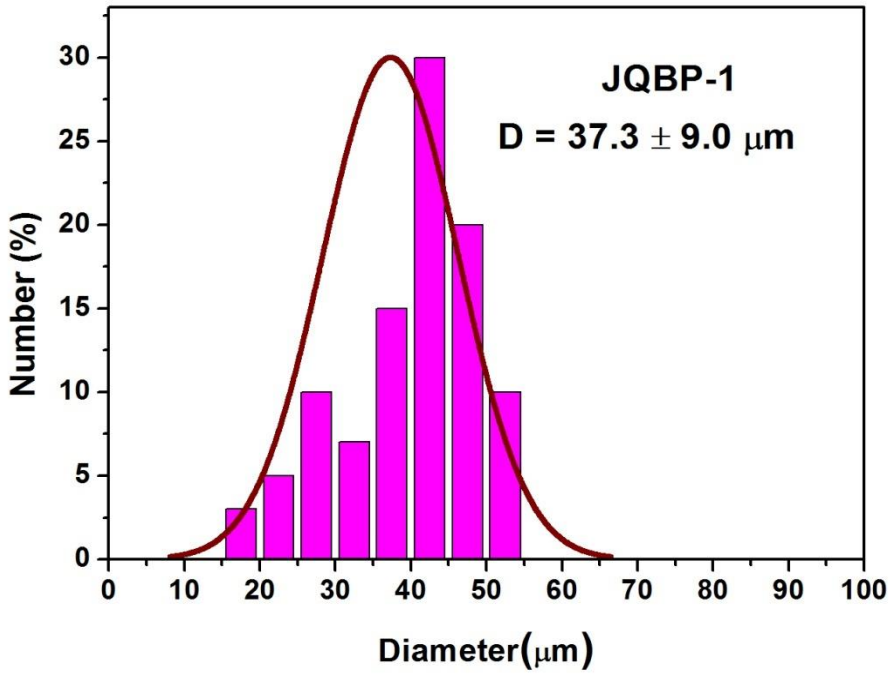

Figure S23. Size distribution of JQBP-1 from the statistics of the vesicles in optical photographs.

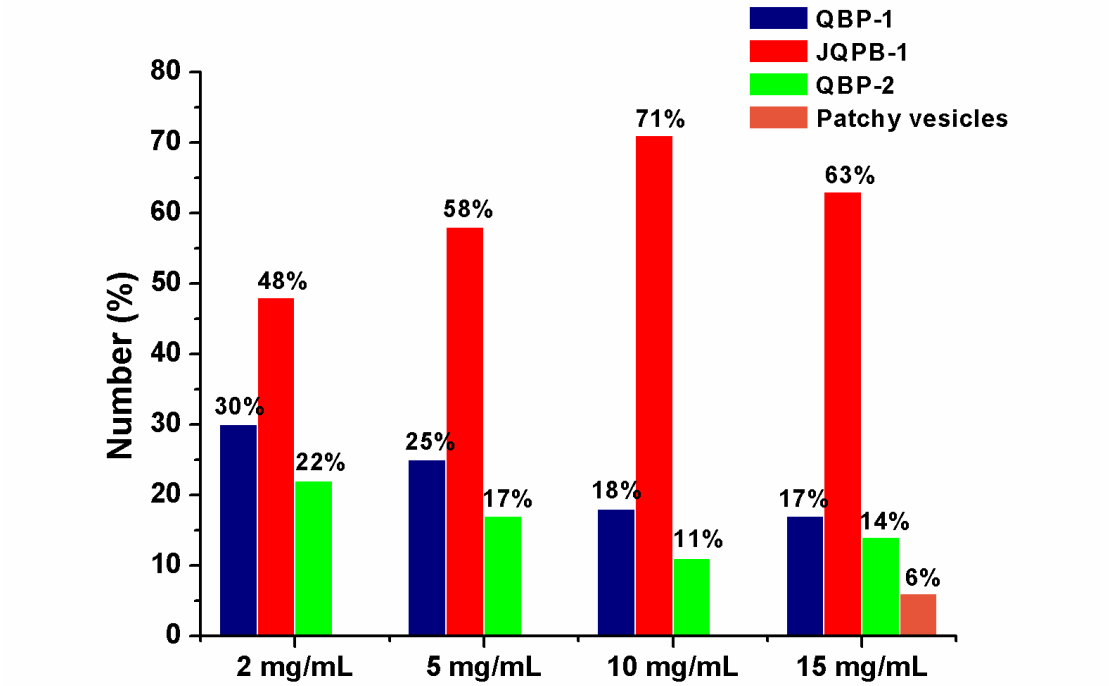

Figure S24. The influence of the hyperbranched polymer concentration on the number percentage of the resultant JQBP-1 (red) in aqueous solution. Data were obtained based on the statistics of the aggregates in fluorescence photographs after the stirring of the mixed vesicle solution for ca. 6 hours.

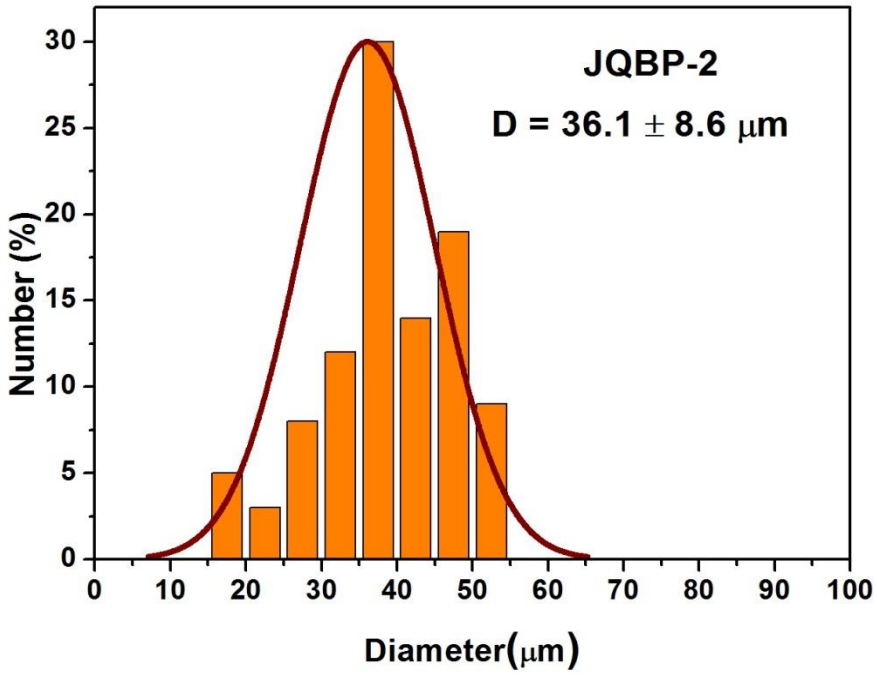

Figure S25. Size distribution of JQBP-2 from the statistics of the vesicles in optical photographs.

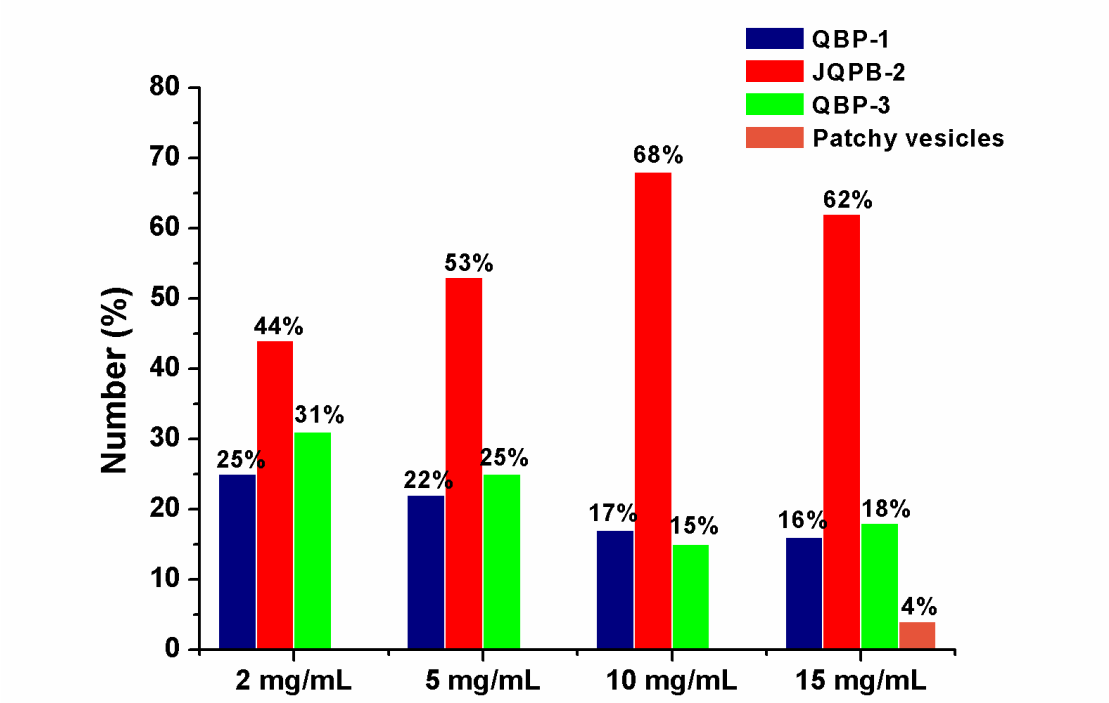

Figure S26. The influence of the hyperbranched polymer concentration on the number percentage of the resultant JQBP-2 (red) in aqueous solution. Data were obtained based on the statistics of the aggregates in fluorescence photographs after the stirring of the mixed vesicle solution for ca. 6 hours.

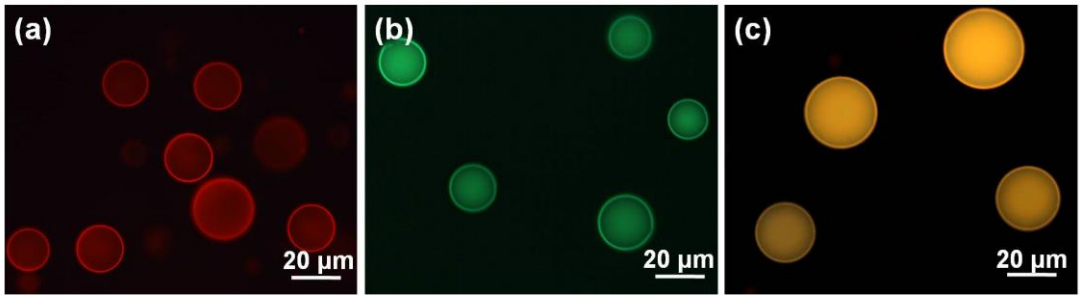

Figure S27. Fluorescence micrographs of BPs incorporated with hydrophobic nile red fluorophore in the wall (a), of BPs with green hydrophobic dansyl chloride in the wall (b), and of the fused vesicles with orange fluorescence (c). All the photos were recorded under fluorescence microscope upon blue light excitation. In this case, no Janus vesicle was observed.

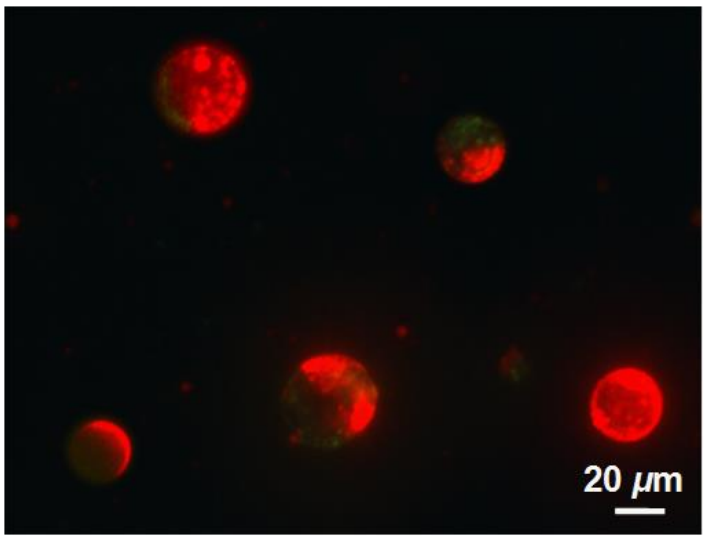

Figure S28. A typical fluorescence image of Janus vesicles prepared by mixing red vesicles containing CdSe/CdS QDs with green vesicles containing dansyl chloride.

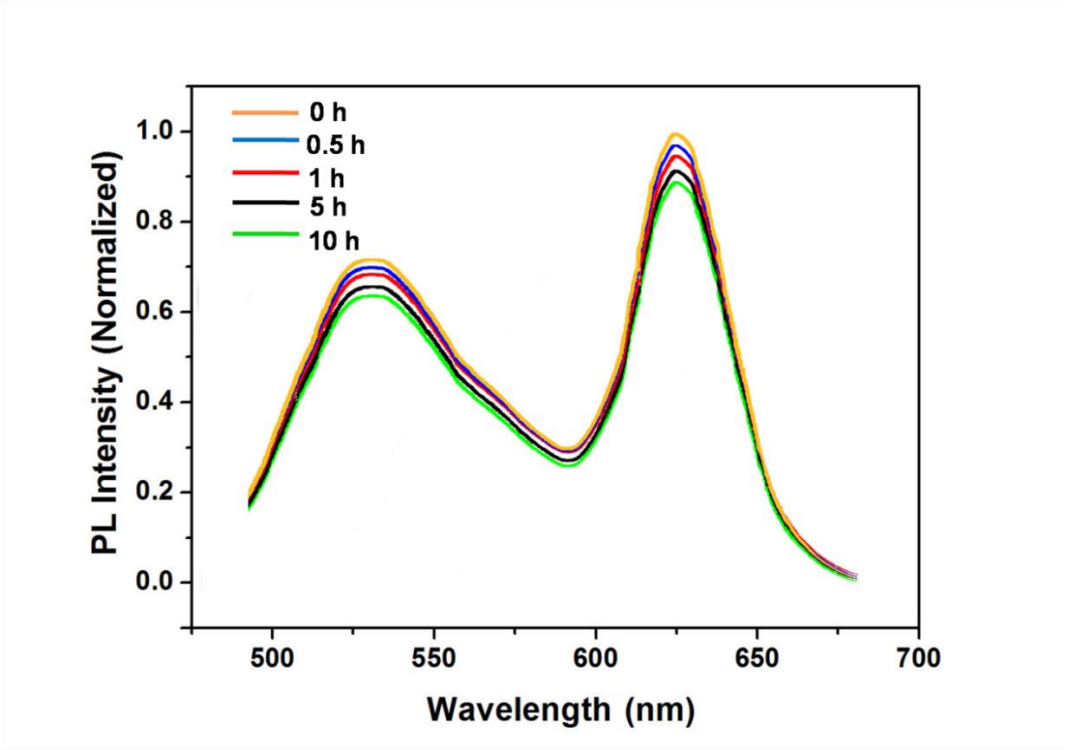

Figure S29. The PL spectra of the mixed solution of QBP-1 and QBP-2, generating JQBP-1, at different aging time.

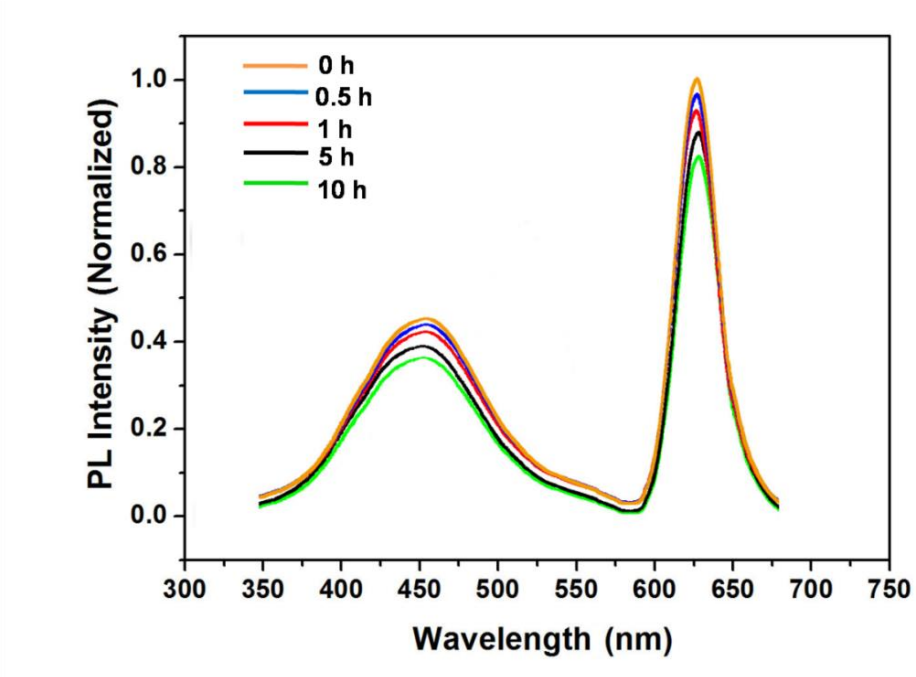

Figure S30. The PL spectra of the mixed solution of QBP-1 and QBP-3, generating JQBP-2, at different aging time.

2.8 *Magnetically-controlled printing of the Janus vesicles*

Several drops of the concentrated JQBP-2 aqueous solutions were dropped on glass slides, then different-letter shaped magnets (e.g. H, I, and L letters) that were made by assembly of commercial magnetic strips were placed under the glass slides to achieve the ordered arrangement of the Janus vesicles. The photos and the movie of the letters upon the excitation by a UV lamp (365 nm) were taken by a digital camera. The fluorescence micrographs of the Janus vesicles in some parts of the letters were taken under an optical/fluorescence microscope (Leica DM4500 B).

In the presence of the magnets, the JQBPs-2 spontaneously patterned into a red-fluorescent letter of "H" (Figure 4 in the main text) and "I" or "L" (Figure S31) upon UV excitation with their Fe_3O_4-containing hemispheres facing down and red CdSe/CdS QD hemispheres facing up. The withdrawal of the magnets resulted in the disordered arrangement of the Janus vesicles, which gave rise to the disappearance of the fluorescent letters.

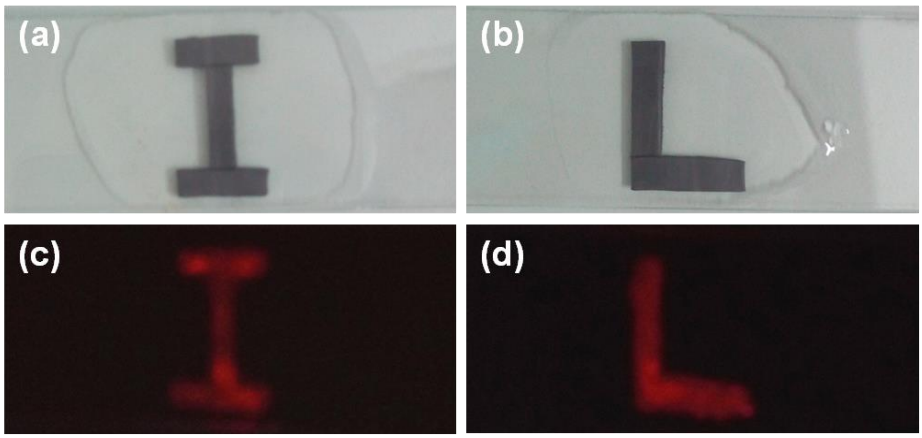

Figure S31. The digital photos of different-letter shaped magnets under the concentrated JQBP-2 aqueous solution (a and b) and their corresponding fluorescence photographs upon UV excitation (c and d).

References

1. Y. F. Zhou and D. Y. Yan, *Angew. Chem. Int. Ed.*, 2004, **43**, 4896; *Angew. Chem.*, 2004, **116**, 5004.

2. Y. Y. Mai, Y. F. Zhou and D. Y. Yan, *Small*, 2007, **3**, 1170.

3. H. B. Jin, Y. L. Zheng, Y. Liu, H. X. Cheng, Y. F. Zhou and D. Y. Yan, *Angew. Chem. Int. Ed.*, 2011**, 50**, 10352; *Angew. Chem.*, 2011, **123**, 10536.

4. H. B. Jin, Y. Liu, Y. L. Zheng, W. Huang, Y. F. Zhou and D. Y. Yan, *Langmuir*, 2012**, 28**, 2066.

5. J. Park, K. An, Y. Hwang, J. G. Park, H. J. Noh, J. Y. Kim, J. H. Park, N. M. Hwang and T. Hyeon, *Nat. Mater.*, 2004**, 3**, 891.

6. R. J. Hickey, X. Meng, P. Zhang and S. Park, *ACS Nano*, 2013, **7**, 5824.

7. R. J. Hickey, A. S. Haynes, J. M. Kikkawa and S. Park, *J. Am. Chem. Soc.*, 2011**, 133**, 1517.

8. A. D. Zhang, Y. Bian, J. Wang, K. Chen, C. Q. Dong and J. C. Ren, *Nanoscale*, 2016**, 8**, 5006.

9. W. W. Yu, L. Qu, W. Guo and X. Peng, *Chem. Mater.*, 2003, **15**, 2854.

10. A. D. Zhang, Dong, C. Q. L. Li, J. Yin, H. Liu, X. Huang and J. C. Ren, *Sci. Rep.*, 2015**, 5**, 15227.